THEORY AND MODELING OF THIN FILM FLOWS

T

S.B.G. O'Brien
University of Limerick, Ireland

L.W. Schwartz
University of Delaware, Newark, Delaware, U.S.A.

INTRODUCTION

Thin liquid films are ubiquitous in nature and technology so an understanding of their mechanics is important in many applications. A typical thin film flow consists of an expanse of liquid partially bounded by a solid substrate with a (free) surface where the liquid is exposed to another fluid (usually a gas and most often air in applications). Typically, the thickness, H, in one direction is much smaller than the characteristic length scale, L, in the other directions and the flow takes place predominantly in the direction of one of the longer dimensions under the action of an external forcing (e.g., gravity, surface tension gradients, a rotating substrate). A simple and obvious example is the flow of a (thin) raindrop down a windowpane under the action of gravity. Typically, the flow velocity in directions perpendicular to the substrate (i.e., the window-pane) is much smaller than the main flow velocity along the windowpane. The most ''correct'' approach to modeling such flows is via the macroscopic momentum equation (e.g., the Stokes or Navier Stokes equations in the case of a Newtonian liquid) and this approach invariably involves detailed numerical computation e.g., Refs. 1 and 2. The approach taken here will be to exploit the existence of the small aspect ratio ($\epsilon \equiv H/L$) to expand the momentum equations in a perturbation series in powers of ϵ. In doing so we will be developing a so-called thin film or long wave approximation (3) with the advantage that analytic solutions will often be possible and where this is not feasible, the reduced numerical problem will be greatly simplified (4). The approximation has much in common with classical lubrication theory (5, 6) and is thus also referred to as the lubrication approximation. The success of this approximation is well documented in the literature and a feature of this success is its robustness (9) and a tendency for it to deliver good results (in agreement with experiment) in parameter regimes on the outer limits of the expected range of validity or beyond. From a mathematical point of view, a typical complication associated with thin film flows is the fact that the free surface of the liquid is initially unknown and must be determined as part of the solution.

In many practical thin film models surface tension plays a significant role (10). Even when formally small, surface tension often has a significant smoothing effect preventing the formation of shocks (sharp jumps in the film thickness). Mathematical models will be given here for flows on flat and curved surfaces including other effects such as gravity, compositional changes, and substrate energetics. Application areas include flow behavior of paints and other surface coatings, chemical, and nuclear reactor design, agrochemical applications, as well as several biofluid applications including thin films on the cornea and in the lungs.

Asymptotic derivations of lubrication theory for 2-D problems with a free surface are given by Benney (3) without surface tension and by Atherton and Homsy (7) where surface tension is included. The thin film approximation can also be applied to non-Newtonian flows and there are many examples in the literature, e.g., Ref. 8.

This article is organized as follows: In THE IDEA BEHIND THE THIN FILM APPROXIMATION we discuss a particular (simple) problem to show how the thin film approximation is applied. Then we will discuss variations on the standard problem and more complicated situations. We then sketch a number of relevant examples in EXAMPLES USING THIN FILM MODELS before making some closing remarks.

THE IDEA BEHIND THE THIN FILM APPROXIMATION

In order to elucidate the basic approximation technique we will consider the particular example of the motion of an incompressible Newtonian thin liquid film down a window pane. The liquid film is assumed to be of large extent with constant density, ρ, dynamic viscosity, μ (kin-

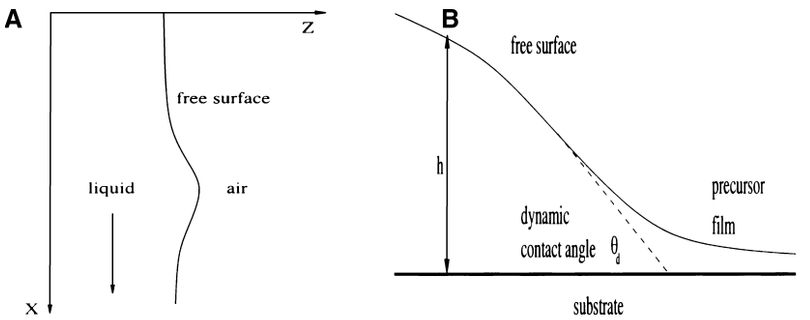

Fig. 1 (**A**) Thin film flow down a windowpane. (**B**) Dynamic contact angle, apparent contact line and precursor film.

ematic viscosity, v), and surface tension, σ. The liquid velocity vector is $\mathbf{u}\ (x, z, t) = (u, w)$, the pressure is $p\ (x, z, t)$, and the film free surface is given by $z = h(x, t)$ in Cartesian coordinates where t is time (Fig. 1A). The gravity vector is given by $\mathbf{g} = (g_x, g_y)$. The variable h must be determined as part of the solution of this problem though $h(x, 0)$ must be prescribed, i.e., we cannot hope to find the subsequent film shape without knowing the configuration at the beginning. We now nondimensionalize (or scale) the problem to bring out balances which reflect the lubrication approximation: derivatives in the x direction should be much smaller than derivatives in the z direction. To this end we introduce dimensionless starred variables as follows:

$$x = x^*L,\ z = z^*H,\ u = u^*U,\ w = w^*W,$$
$$p = p^*\frac{\mu UL}{H^2},\ t = t^*L/U \tag{1}$$

where L is a length scale associated with $O(1)$ changes in the flow velocity in the direction of the main flow, H is typical film thickness,

$$U \equiv \frac{\rho g H^2}{\mu}$$

and W is a typical velocity in the z direction. The stress tensor is also nondimensionalized via

$$\mathbf{T} = \mathbf{T}^*\frac{\mu UL}{H^2},$$

and we find that

$$T^*_{11} = -p^* + 2\epsilon^2\frac{\partial u^*}{\partial x^*};$$
$$T^*_{12} = T^*_{21} = \epsilon\frac{\partial u^*}{\partial z^*} + \epsilon^3\frac{\partial w^*}{\partial x^*};$$
$$T^*_{22} = -p^* + 2\epsilon^2\frac{\partial w^*}{\partial z^*} \tag{2}$$

where $\epsilon \equiv H/L << 1$. Thus $T^*_{ij} = -p^*\delta_{ij} + O(\epsilon)$ regardless of the velocity scale U being used. The normal stresses dominate as in classical lubrication theory (5). The scaled mathematical problem now becomes

$$\epsilon^2 Re\left(\frac{\partial u^*}{\partial t^*} + u^*\frac{\partial u^*}{\partial x^*} + w^*\frac{\partial u^*}{\partial z^*}\right) = -\frac{\partial p^*}{\partial x^*} + \epsilon^2\frac{\partial^2 u^*}{\partial x^{*2}} + \frac{\partial^2 u^*}{\partial z^{*2}} + \bar{g}_x \tag{3}$$

$$\epsilon^4 Re\left(\frac{\partial w^*}{\partial t^*} + u^*\frac{\partial w^*}{\partial x^*} + w^*\frac{\partial w^*}{\partial z^*}\right) = -\frac{\partial p^*}{\partial z^*} + \epsilon^4\frac{\partial^2 w^*}{\partial x^{*2}} + \epsilon^2\frac{\partial^2 w^*}{\partial z^{*2}} + \bar{g}_z \tag{4}$$

$$\frac{\partial u^*}{\partial x^*} + \frac{W}{\epsilon U}\frac{\partial w^*}{\partial z^*} = 0 \tag{5}$$

where

$$\bar{g}_x = g_x\frac{H^2}{vU},\quad \bar{g}_z = g_z\frac{H^3}{vUL},$$

and

$$Re = \frac{UL}{v}.$$

The latter term is the traditional Reynolds' number but the actual Reynolds' number (i.e., the ratio of inertia and viscous terms) for thin film flow is $\epsilon^2 Re$. In the particular problem under consideration $g_x = g$, $g_z = 0$ where g is the scalar acceleration due to gravity. With the scale

$$U = \frac{\rho g H^2}{\mu}$$

we then find that $\bar{g}_x = 1$, $\bar{g}_z = 0$. In deducing the scales (Eq. 1), the following considerations were important: In Eq. 3 the driving force is the gravity term and we would expect the viscous forces and the gravity term to be of the same order; the scale for the pressure was chosen by assuming that in the absence of further information the pressure term in Eq. 3 was also of the same order as the gravity term. (In this formulation, surface tension effects are assumed ''small'' and will enter at the next order, although we elaborate on this point later. If surface tension dominates, then an alternative velocity scale

$$U = \frac{\sigma H^3}{\mu L^3}$$

should be used.) If the scales chosen are relevant we can now identify the dominant terms/effects in the problem. From Eq. 5, assuming the two terms balance we deduce that $W = \epsilon U$, i.e., the typical velocity in the z direction is much smaller than that in the x direction.

The scaled boundary conditions (no slip and no penetration) take the form

$$u^* = w^* = 0 \text{ on } z^* = 0 \tag{6}$$

If the (unknown) free surface is $z^* = h^*(x^*, t^*)$, the normal and tangential vectors and the surface curvature κ can be written as

$$\begin{aligned}
\hat{\mathbf{n}} &= \left(-\epsilon h^*_{x^*}, 1\right)\left(1+\epsilon^2 h^{*2}_{x^*}\right)^{-\frac{1}{2}};\\
\hat{\mathbf{t}} &= \left(1, \epsilon h^*_{x^*}\right)\left(1+\epsilon^2 h^{*2}_{x^*}\right)^{-\frac{1}{2}};\\
\kappa &= \frac{\epsilon}{L} h^*_{x^*x^*}\left(1+\epsilon^2 h^{*2}_{x^*}\right)^{-\frac{3}{2}}
\end{aligned} \tag{7}$$

while on the free surface we have

$$\hat{\mathbf{n}} \cdot \mathbf{T}^* \cdot \hat{\mathbf{n}} = \frac{\epsilon^3}{Ca}\kappa^* \tag{8}$$

$$\mathbf{T}^* \cdot \hat{\mathbf{n}} - \frac{\epsilon^3}{Ca}\kappa^* \hat{\mathbf{n}} = 0 \text{ i.e., } \hat{\mathbf{t}} \cdot \mathbf{T}^* \cdot \hat{\mathbf{n}} = 0 \tag{9}$$

on $z^* = h^*(x, t)$. Here $\kappa = \epsilon\kappa^*/L$ defines a scaled free surface curvature, $Ca = \mu U/\sigma$ is a capillary number (which can also be interpreted as a Bond number with the chosen velocity scale $U = \rho g H^2/\mu$, i.e., $Ca = \rho g H^2/\sigma$). The first of these conditions reflects the fact that a (massless) curved interface in equilibrium must give rise to a jump in the pressure via the surface tension as the interface is crossed. Both conditions assume that the gas exerts a negligible shear stress on the liquid, although more general conditions can be applied in the case of a liquid–liquid interface (6). If the location of the free boundary were known, we would now have a well-posed mathematical problem. Instead, we require an extra condition on the free boundary, the scaled kinematic condition, which takes the form

$$\frac{D(z^* - h^*)}{Dt^*} = 0$$

on $z^* = h^*$ where D/Dt^* is the convective derivative. This may be written as

$$\begin{aligned}
w^* &= \frac{\partial h^*}{\partial t^*} + u^* \frac{\partial h^*}{\partial x^*} \text{ or } \frac{\partial h^*}{\partial t^*} = -\frac{\partial Q^*}{\partial x^*};\\
Q^* &= \int_{z^*=0}^{z^*=h^*} u^* dz^*
\end{aligned} \tag{10}$$

on $z^* = h^*(x^*, t^*)$ where the liquid flux or volume rate of flow has been scaled via $Q = UHQ^*$. The thin film approximation can now be obtained by taking the limit of Eqs. 3–5 as $\epsilon \to 0$ while assuming other parameters are $O(1)$. Thus we have

$$\frac{\partial p^*}{\partial x^*} = \frac{\partial^2 u^*}{\partial z^{*2}} + 1; \quad \frac{\partial p^*}{\partial z^*} = 0; \quad \frac{\partial u^*}{\partial x^*} + \frac{\partial w^*}{\partial z^*} = 0 \tag{11}$$

The success of these equations from a mathematical point of view depends on the fact that $p^* = p^*(x^*, t^*)$ allowing the first equation to be integrated to yield

$$u^* = \left(\frac{\partial p^*}{\partial x^*} - 1\right) z^{*2}/2 + Az^* + B$$

where the constants of integration A, B are determined from the boundary conditions. In the present case we find using Eq. 8 to leading order that p^* and hence $p^*_{x^*}$ is zero everywhere and it follows that

$$u^* = h^* z^* - \frac{1}{2} z^{*2}; \quad w^* = -\frac{\partial h^*}{\partial x^*} z^{*2}$$

The kinematic condition, Eq. 10, now yields an evolution equation for $h^*(x^*, t^*)$, i.e.,

$$\frac{\partial h^*}{\partial t^*} + h^{*2} \frac{\partial h^*}{\partial x^*} = 0$$

This first-order quasilinear partial differential equation requires an initial condition (modeling the initial configuration of the liquid film), e.g., $h^*(x^*, 0) = f(x^*)$ where

$f(x^*)$ is a known function. Using the method of characteristics, the implicit solution is $h^* = f(x^* - h^{*2}t^*)$.

Wave Steepening and Shocks

In the present example we have assumed that surface tension effects are ''small.'' Solutions of the form $h^* = f(x^* - h^{*2}t^*)$ are known to develop shocks (i.e., sharp jumps in h^*) if the initial condition $f(x^*)$ is ever decreasing. This describes a nonlinear wave motion, with typical steeping at the front of the wave and eventual wave breaking. In practice, such wave breaking is not observed and the perturbation is a singular one in that when the wave becomes sufficiently steep some of the formally small higher derivative terms of the leading order lubrication approximation can become significant. Referring to Eq. 8 we note that the right hand side is $O(\epsilon^3/Ca)$; where

$$Ca = \frac{\mu U}{\sigma} = \frac{\rho g H^2}{\sigma}$$

We can develop an improved lubrication approximation if $Ca \leq O(\epsilon)$ in which case we can write $Ca = \overline{Ca}\epsilon$ where $\overline{Ca} \leq O(1)$. When wave steepening occurs we introduce a rescaled ξ coordinate defined as

$$x^* - x_s(t) = \delta\xi \tag{12}$$

where $x_s^*(t)$ is the speed of the shock that develops as a solution of the zero-order (hyperbolic) problem. When we rescale in this fashion and repeat our previous development, we obtain the following boundary layer equation to leading order:

$$-\frac{1}{\delta}\frac{dx_s}{dt^*}h_\xi^* + \frac{1}{\delta}h^{*2}h_\xi^* = \frac{\epsilon^2}{3\delta^4\overline{Ca}}\left(h^{*3}h_\xi^*\right)_\xi \tag{13}$$

Thus, the surface tension terms become significant when $\delta = O(\epsilon^{2/3})$, which defines the boundary layer thickness. Note that the slope of the free surface (in the boundary layer) is still ''small,'' as $h_x = O(\epsilon^{1/3})$. Furthermore, an examination of Eqs. 8 and 9 indicates that the surface tension terms of Eq. 8 are the dominant first order terms in this improved lubrication approximation. In the circumstances, we can use an improved evolution equation:

$$\frac{\partial h^*}{\partial t^*} + h^{*2}\frac{\partial h^*}{\partial x^*} = \frac{\epsilon^2}{3\overline{Ca}}\frac{\partial}{\partial x^*}\left(h^{*3}\frac{\partial h^{*3}}{\partial x^{*3}}\right) \tag{14}$$

and numerically examine this equation. Analytic solutions are usually out of the question here (although similarity solutions are sometimes possible) but it is well known that the higher derivative terms have a smoothing effect on solutions, wave steeping occurs, but wave breaking is inhibited. Of course, we can also treat Eq. 14 as a singular perturbation problem, solve the outer problem in closed form; and match this to an inner solution. If the parameter $\epsilon^2/\overline{Ca}(\epsilon^3/Ca)$ is small in practice, it is often worthwhile to consider the reduced equation obtained by neglecting the higher derivative terms as the simplified problem can be analyzed using the method of characteristics though wave breaking, if it occurs, must then be resolved by the insertion of suitable shock discontinuities.

It is the common practice of many authors to preferentially promote (i.e., rescale) the surface tension terms so that they are $O(1)$, i.e., by assuming that $\epsilon^3/Ca = O(1)$. Whether or not this is technically correct depends on the particular parameter values in the problem under consideration but the philosophy is that even if these terms are everywhere small, including them will still give a correct approximation to leading order and usually has the desirable effect of making the numerical technique more stable.

In the small slope approximation, the dimensional pressure in the liquid layer of thickness $h(x, y, t)$ lying on a 2-D planar substrate, relative to the air above, will include a surface tension contribution $p^{(\sigma)} = -\sigma\nabla^2 h$. If gravity is also important, the specific form of the gravity contribution to p depends on the orientation of each substrate element. Thus, if gravity is also considered, we state that typical substrate scale lengths are of the order

$$L_c = \sqrt{\frac{\sigma}{\rho g}},$$

the so-called capillary length. Therefore, practically speaking, we are more concerned with flow on centimeter-scale objects rather than meter-scale objects in terrestrial gravity. Of course, if gravitational acceleration is very small, as in space shuttle experiments, for example, capillary effects become important at larger physical dimensions.

In the remainder of this article, following common practice in the thin film literature, we will generally write equations in terms of dimensional variables (an asterisk denotes a dimensionless variable) although it is tacitly understood that a formal scaling process has been carried out for each problem in order to obtain the leading order balances. Once this has been achieved, the equations are then rewritten in terms of the original dimensional variables with the advantage that is often easier to identify the physical significance of particular terms.

Moving Contact Lines

In ''The Idea Behind the Thin Film Approximation,'' we considered the flow of a continuous film under gravity. An obvious related problem is to consider the flow of an isolated drop of liquid over an otherwise dry substance. In this case, a three-phase line appears at the front of the droplet where liquid, gas, and solid meet. If a no-slip boundary condition is enforced at the three-phase line and there is relative motion between the liquid and the solid, a nonintegrable singularity occurs in the stress at the three-phase line signifying an unphysical infinite force (11). The continuum hypothesis fails in the neighborhood of the contact line and some mechanism must be introduced to relieve the infinite force. One possibility is to introduce a Navier slip boundary condition (12) on the substrate surface, which in the lubrication approximation for 2-D flow takes the form

$$\beta u = \mu \frac{\partial u}{\partial z} \tag{15}$$

where μ/β is referred to as the slip length. Thus, the slip velocity is proportional to the shear stress. Typically, μ/β is very small (of the order of molecular length scales) and the condition reduces to $u \approx 0$, except in the immediate neighborhood of the contact line where $\partial u/\partial z$ becomes large. It is a matter of experience that the choice of slip condition and slip length does not significantly affect the dynamics of the flow in the region away from the contact line (13). When surface tension plays a significant role, a boundary condition is needed at the contact line in terms of the contact angle, but there is little agreement in the literature as to how this should be done. For the case of very slow flow, a quasi-static approach can be used (14, 15). Outside this regime, the interface can be considerably deformed via viscous effects in the vicinity of the contact line. Thus, the so-called apparent (a.k.a., dynamic or observed) contact angle, θ_d, i.e., the slope of the free surface measured a short distance from the contact line, can be significantly different from the contact angle, θ_c, measured at the contact line (if such a line really exists) (Fig. 1B). *The dynamic contact angle is thus a local observation for a particular problem, at a particular point on the moving contact line.* In addition, the dynamic contact angle exhibits hysteresis and is a function of the speed with which the contact line moves relative to the substrate. For modeling purposes, when using the notion of a contact angle there are two main schools of thought (16): The first school uses the static or equilibrium value of the contact angle, $\theta_c = \theta_e$, (even when the contact line is moving) and a slip boundary condition. The second uses a dynamic contact angle, θ_d, measured at some known distance from the contact line. The idea is that θ_d is not a material constant but can be measured experimentally for each problem as a function of contact line speed at a particular distance from the contact line. Once this has been done, the dynamics in the inner region can be ignored — its effect on the outer region is contained in the value of this angle (17). This concept is really only suitable for flows with a high degree of symmetry for which a dynamic contact angle can unambiguously be defined.

One can attempt to explore the physics of the fluids near the contact line by investigating the dynamics of several thousand atoms modeled using a Lennard–Jones type potential (18). Solutions in agreement with the Navier–Stokes equation were obtained with a no-slip boundary condition except within about two atomic spacings of the moving contact line where slip occurred. While this might seem to verify the plausibility of using a slip boundary condition near a contact line, one can query whether using a Lennard–Jones potential accurately represents the physics.

The simplest practical technique for modeling moving contact lines, and one which we recommend, is to ignore all reference to dynamic contact angles and use the notion of a very thin precursor film ahead of the contact line (Fig. 1B) whose thickness, h_p, is assumed constant and known (see Finite Contact Angle Effects, Wetting, and Dewetting). This has the advantage of removing the difficulty arising at the contact line so that a no-slip condition can be applied everywhere. In addition, the outer dynamics turn out to be only weakly dependent on the choice of precursor film thickness (19, 20). For the case of a volatile liquid (e.g., water) it has been demonstrated that spreading rates increase with humidity (21), which is consistent with the notion of the precursor film. For the case of a non-volatile film, the insertion of a precursor of known thickness in effect introduces a slip layer. The smaller the thickness of this layer, the harder it is to move the contact line. Whether such a layer is real or not is not the issue: The precursor film thickness, h_p, is an adjustable or free parameter but so too is the slip length in the Navier model (Eq. 15). Both mechanisms relieve the stress singularity.

To date, there is no general agreement on the best way to model moving contact lines, but we suggest that the precursor film technique will stand the test of time. The success or failure of moving contact line models must ultimately rest on comparison with observation.

The quasi-steady state analysis of Tanner (22) for the spreading of an axisymmetric drop is worthy of note and leads, in the lubrication limit using essentially a precursor film, to an explicit model for the dynamic contact angle

and a prediction of the drop radius, R, as a function of time, i.e., $R(t) \sim t^{0.1}$ in excellent agreement with experimental results.

Surface Tension Gradients and the Marangoni Effect

Up to this point we have considered only models with constant surface tension. Many liquids (e.g., water) have a surface tension that can be varied by the addition of so-called surface active substances (surfactants). These are substances that tend to congregate in the upper layers of the liquid, changing its surface energy and hence its surface tension. For example, soap lowers the surface tension of water, which is why we use it while washing. Surfactants introduce the possibility of generating a surface tension gradient, resulting in a shear stress on the liquid free surface (23). In such cases, the tangential stress condition of Eq. 9 is modified as follows:

$$\mathbf{T}\cdot\mathbf{n} - \mathbf{n}\,\sigma(C)\kappa = \nabla_S\sigma(C) \tag{16}$$

where $\nabla_S = (\mathbf{I} - \mathbf{nn})\nabla$ is the surface gradient operator and σ(c) is the concentration dependent surface tension. If we consider a 2-D problem uniform in the y direction, this reduces in a leading order thin film approximation to the simple form

$$\mu\frac{\partial u}{\partial z} = \frac{\partial \sigma}{\partial x}$$

Models for such flows may also require modeling of the transport of solute in the liquid phase and, generally speaking, the liquid and solute transport are strongly coupled. Marangoni effects can also be induced via temperature gradients in the liquid as surface tension tends to be a weak function of the temperature, T, in which case $\sigma = \sigma(T)$.

Flow Over Nonflat Substances

In some technological processes, in particular coating processes, a thin film is applied to a flat substrate with some localized defect (or topography) or to a substrate with intrinsic curvature, e.g., a television screen. For example, the laying down of phosphor patterns on the inside of a television screen is a multi-step process. During the later stages, coatings are laid down on screens already containing a particular topography of partially etched phosphor dots. Though this is a spin coating–type process, the modeling is similar to the basic model shown in THE IDEA BEHIND THE THIN FILM APPROXIMATION. Surface tension can play a significant role in the neighborhood of the surface features. The lubrication approximation has been extensively used to model such situations, even in the case where the curvature of the underlying topography is quite extreme (for example, consisting of steps). Although such flows, strictly speaking, fall outside the range of validity of thin film theory, good results have been obtained in agreement with experimental results (24). Of particular interest is the modeling of thin film flows on curved surfaces. Generally speaking, surface tension effects tend to flatten a film (to reduce curvature), thus producing a level film. This beneficial effect of surface tension is limited largely to substrates where curvature variation is small. If a substrate has relatively high curvature, surface tension can result in defects in the final coating: This results in a coating that is too thin at outside corners and too thick at inside corners.

The thin film approximation for flow along a curved substrate is still valid provided the typical film thickness satisfies $H << R$, where R is the local radius of curvature of the substrate (in the 2-D case) (25). In applications, H tends to be very small. For example, if $H << 1$ mm then the thin film approximation is still valid for substrates with curvatures as large as $10^3\mathrm{m}^{-1}$ (25). Using a local orthogonal coordinate system (s, n) where s is arc length along the substrate and $n = h(x,t)$ is the layer thickness, to be determined, a local force balance is used to obtain a thin film approximation. Surface tension is included by writing the film curvature as a perturbation of the underlying substrate curvature. Thus, if the local radius of curvature of the substrate (with its center of curvature taken to be on the opposite side from the liquid film) is $R(s)$, the curvature, $\kappa(s)$, of the free surface is approximated as

$$\kappa(s) \approx \frac{1}{(h+R)} + \frac{\partial^2 h}{\partial s^2} \approx \frac{1}{R}\left(1 - \frac{h}{R}\right) + \frac{\partial^2 h}{\partial s^2} \tag{17}$$

where we have included a term, h/R^2, that was omitted previously (25). [There is an obvious generalization $\kappa \approx 1/R_1 + 1/R_2 - h(1/R_1^2 + 1/R_2^2) + \nabla^2 h$ for the 3-D case where R_1, R_2 are the principal radii of curvature]. With this insight, the development of a thin film evolution equation for $h(s, t)$ is straightforward and takes the form

$$h_t = -\frac{\sigma}{3\mu}\left((h^3(\kappa_s)\right)_s \tag{18}$$

EXAMPLES USING THIN FILM MODELS

Finite Contact Angle Effects, Wetting, and Dewetting

Motion of liquids onto or from dry substrate areas requires special treatment. Such contact-line motions con-

tradict the usual no-slip boundary condition and a degree of ''slip'' must be introduced. Often the dry areas are due to lack of perfect wetting, as reflected in finite values of measurable contact angle. Both the required slip and the ability to prescribe an equilibrium contact angle are enabled by using a ''disjoining'' pressure term in the evolution equation. The pressure in the liquid is now given by

$$p = -\sigma\kappa - \Pi \approx -\sigma\nabla^2 h - \Pi \tag{19}$$

within the small surface slope approximation. A two-term disjoining pressure is consistent with the Frumkin–Derjaguin model that relates static contact angles to interfacial energies and also can be used in dynamical cases (26, 28):

$$\Pi = B\left[\left(\frac{h_p}{h}\right)^n - \left(\frac{h_p}{h}\right)^m\right]. \tag{20}$$

B and the exponents n and m are positive constants with $n > m > 1$. The local disjoining energy density, $e^{(d)}(h) = -\int_{hp}^{h} \Pi(h')\, dh'$, has a single stable energy minimum at a prescribed value, h_p. For nominally dry substrates, the precursor film thickness (see Moving Contact Lines), h_p, plays the role of a slip coefficient, as required to overcome the moving contact line force singularity. The quantity, B, may be related to the equilibrium contact angle, θ_e, using $\sigma \cos \theta_e = \sigma - e^{(d)}(\infty)$, which is the disjoining model equivalent of the Young equation. $\theta_e(x, y)$ can be a prescribed ''wettability'' pattern on the substrate. In such cases, B in Eq. 20 is also a function of position. When Π is appended to the free surface evolution equation, a variety of problems on partially covered substrates can be treated. The exponent pair, (n, m), controls the shape of the disjoining energy ''well'' at $h = h_p$.

The model can be calibrated by comparison with several experiments. For complete wetting ($\theta_e = 0$), Tanner's (22) measurements of power-law spreading rates for an axisymmetric droplet are reproduced using realistically small values of h_p. Droplet spreading simulations at finite contact angle on a homogeneous substrate ($\theta_e = constant > 0$) show agreement with the experimental observations of Zosel (29).

In laboratory experiments (27), a 26-μl drop of glycerin was placed near the center of a cross of 1 mm Teflon tape that had been fixed to a horizontal glass slide. Wetting forces cause the drop to break up into unequal fragments. Simulation results show detailed agreement with the experiment (Fig. 2) (27). However, timescale corrections need to be applied because 1) the simulation precursor layer, h_p, is overly large due to computational limitations, and 2) the contact angles in the experiment are beyond the range of quantitative validity of the small-slope lubrication approximation. In both the experiment and the simulation, the motion proceeds in a ''jerky'' manner that is characteristic of capillary driven motions on nonuniform substrates.

Simulation of contact angle hysteresis

Simulations have been performed to investigate the origin of ''contact angle hysteresis,'' an effect associated with the dissipation of energy when a liquid moves on mixed-wettable substrates. Periodic square patch patterns of ''grease,'' i.e., high-contact-angle material, are used. We consider the motion of a drop, both in spontaneous motion, driven only by wetting forces, and also in a periodic forced motion. In spontaneous motion, the droplet edge can ''hang up,'' either permanently or for long times, on the grease spots, as shown in Fig. 3A (28). Quantitative measures of contact angle hysteresis (CAH) can be extracted from the numerical results and related to the defect pattern. CAH is a gross measure of the degree of imperfection of the substrate and is a characteristic of all real materials.

A global energy balance equation may be written for this system, $\dot{E}^{(\mu)} = -(\dot{E}^{(\sigma)} + \dot{E}^{(d)}) + W$, where the terms represent, respectively, the rate of viscous dissipation, the rates of change of capillary and disjoining energy, and the rate of working by injection forces (if present), each inte-

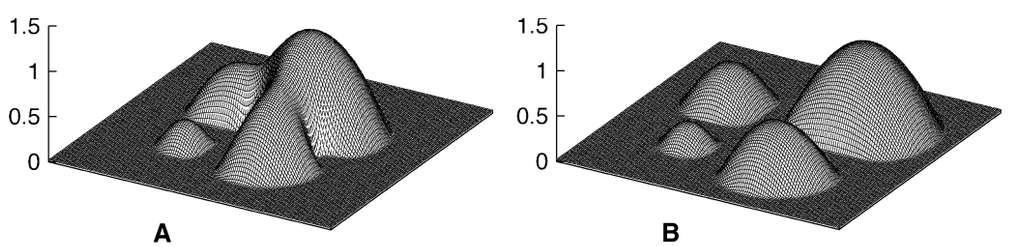

Fig. 2 Time-dependent evolution of a drop placed near the center of a cross of poor-wetting material. (**A**) $t = 0.35$ (dimensionless). (**B**) $t = 0.70$. (©Academic Press.)

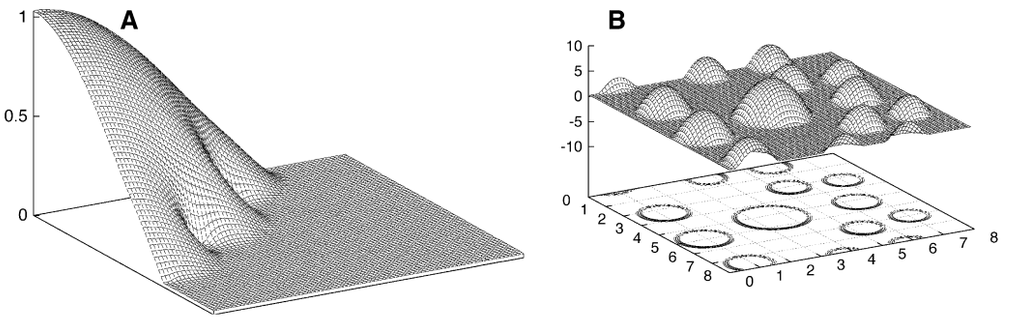

Fig. 3 (**A**) The edges of a drop de-wet on ''grease'' patches. (Reprinted with permission from Ref. 28 ©1998 American Chemical Society.) (**B**) Modeling of spontaneous dewetting. An initially uniform liquid layer, perturbed, breaks into long ridges and then into isolated droplets.

grated over the substrate area. Injection and removal of liquid from a drop, and measurement of the pressure, as the volume is varied, can be used to probe the dynamic effect of particular substrate wettability patterns. In that case the total viscous work done is the time integral of W, i.e., $p\,dV$, where V is drop volume, $dV = w_i\,dA$, and the special integral sign denotes a full cycle. The term $w_i(x, y, t)$ is the imposed injection velocity distribution.

Dewetting

Dewetting is a ubiquitous phenomenon that is easily observed and often undesirable. Certain chemical and nuclear reactors employ wet walls for thermal protection when hot gases are contained under pressure. Dry spots on the walls can lead to catastrophic puncturing. Similarly, dewetting of the tear film in the eye is a potentially serious medical condition. In printing applications, the failure of a nominally uniform coating into a pattern of dewetted spots is called reticulation. Dewetting is sometimes intentional; waxy coatings on leaves of certain plants help them to channel dew and rainwater. The ''balling up'' of water on a freshly polished automobile indicates a high level of rust protection.

We can readily simulate spontaneous dewetting. Either a small localized perturbation or random noise will initiate the dewetting process. We can apply a linear stability analysis to the evolution equation formed by supplementing Eqs. 19 and 20 with mass conservation. An initially uniform layer of thickness $h_0 >> h_p$ can be shown to have a most unstable wavelength proportional to $h_0^{(m+1)/2}$. The corresponding initial disturbance growth rate, proportional to $\sigma\theta_e^4/(\mu h_0^{2m-1})$, is a strong function of equilibrium contact angle, θ_e. A simulation of dewetting is shown in Fig. 3B. The simulation first shows break-up into long ridges which then break up into drops. This two-stage process is also observed in other nonlinear, pattern-formation processes (30).

Pinholing is a phenomenon associated with spontaneous dewetting where small holes can open in a thin film. Consider the case of a thin undisturbed liquid film on a flat substrate. If a defect occurs in the film (for example, a small dirt particle may give rise to a local Marangoni flow and crater formation), the question is whether or not the hole will remain stationary, heal over, or grow. Taylor (31) showed numerically in the static case that corresponding to any film thickness there is precisely one (unstable) axisymmetric hole and proposed that holes smaller than this will heal over, holes larger than this will open out. If we nondimensionalize lengths with the thickness of the layer H, so that the lower solid surface is $z = 1$ and balance the capillary pressure jump across the curved surface with the hydrostatic pressure in the liquid, the equation for the free surface is

$$\mathrm{sgn}(z_r)\left(\frac{z_{rr}}{(1+z_r^2)^{3/2}}+\frac{z_r}{r(\mathrm{I}+z_r^2)^{1/2}}\right)+\epsilon^2 z \;=\; 0$$

Here, $\epsilon^2 = \rho g H^2/\sigma$ is the inverse of the Bond number where H is the undisturbed film thickness. For a 40-μm layer of waterlike coating, $\epsilon \approx 0.07$, which justifies an asymptotic analysis (35). It can be shown (36) that the relationship between the critical dimensionless hole radius, r_0, and the dimensionless film thickness is

$$r_0(\epsilon) = \frac{1}{\ln(1/\epsilon)+\ln(1/r_0)+2\ln(2)-\ln\cot(\theta/2)-\gamma} \tag{21}$$

where γ is Euler's constant. This equation can be solved numerically for a particular film thickness. More recent experience suggests that dynamic effects must be taken

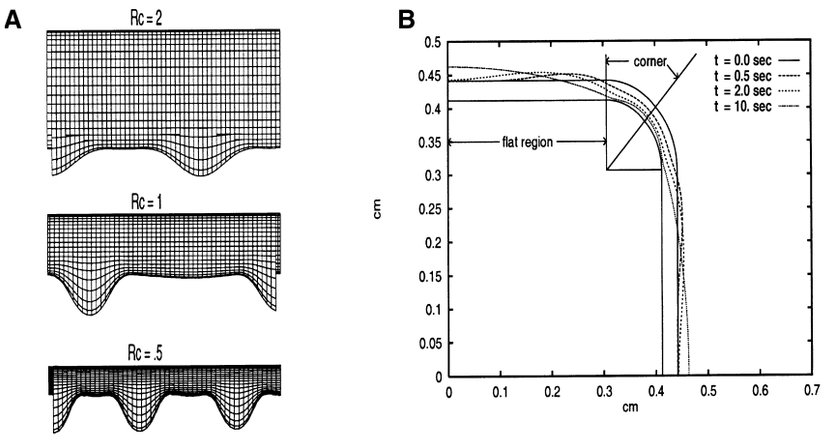

Fig. 4 (**A**) Computed drop shapes hanging from horizontal cylindrical rods. The rod radius is given in units of the capillary length. (©Academic Press.) (**B**) The flow of Newtonian liquid away from an outside corner of radius 0.1 cm and the resulting profile at various times. The thickness of the coating layer is exaggerated for clarity. (With kind permission of Kluwer Academic Publishers.)

into consideration. This has been done in the thin film case (19, 32–34) which suggests that borderline holes that are expected to open from static considerations may, in certain circumstances, not do so. A full Stokes flow model (as distinct from thin film, small slope theory) would be a useful, practical tool.

Treatment of Nonplanar Substrates

The theory of thin layer coating flows may be extended to include flow on substrates that are not flat, as mentioned in THE IDEA BEHIND THE THIN FILM APPROXIMATION.

Substrates of constant mean curvature

For flow on cylindrical or spherical objects, for example, it is possible to reformulate the thin layer equations using a coordinate system that fits the surface. An example of a calculation performed in cylindrical polar coordinates is shown in Fig. 4A (37). The evolution of initially uniform layers of nonevaporating Newtonian liquid on solid horizontal rods of various radii has been found. Ultimately, a pattern of pendant drops forms on the lower side.

In rimming flow, a thin film of viscous liquid is entrained on the inside of a horizontally rotating cylinder at constant angular velocity, ω (38–40).

Using a zero-order thin film approximation the dimensional liquid flux, $q^*(\theta)$, is given by

$$q^* = \omega R h^* - \frac{1}{3}\frac{g}{v}h^{*3}\cos\theta$$

(38). For steady flow, q^* is independent of time, t^*. Using the scales

$$h^* = h\left(\frac{\omega R v}{g}\right)^{\frac{1}{2}}, \quad q^* = q\left(\frac{\omega^3 R^3 v}{g}\right)^{\frac{1}{2}}$$

the equation for the dimensionless flux is

$$q = h - \frac{1}{3}h^3\cos\theta$$

The average dimensional film thickness is given by

$$H_0^* = \frac{1}{2\pi}\int_0^{2\pi} h^* d\theta$$

and this is related to the volume fraction, V, by

$$V = \frac{2RH_0^* - H_0^{*2}}{R^2}$$

The average *dimensionless* film thickness is

$$H_0 = \frac{1}{2\pi}\int_0^{2\pi} h d\theta = \frac{H_0^*}{R}\left(\frac{gR}{\omega v}\right)^{\frac{1}{2}} = \epsilon\,\Omega^{-\frac{1}{2}} \qquad (22)$$

where

$$\Omega \equiv \frac{\omega v}{gR}$$

is a dimensionless rotation rate and

$$\epsilon \equiv \frac{H_0^*}{R}$$

is the aspect ratio (and the small parameter used as a basis for thin film theory). Note that Eq. 22 implies a relationship between q and H_0 (or Ω). H_0 is an $O(1)$ dimensionless parameter, which can be calculated for any particular set of flow parameters and which determines whether or not shocks form. The term q (or q^*) is not a directly adjustable parameter from an experimental point of view. From a theoretical point of view, it is easier to examine solutions to

$$q = h - \frac{1}{3}h^3 \cos\theta,$$

assuming that q is known and to deduce $h(\theta)$ while requiring that Eq. 22 is satisfied. It can be shown (39) that solutions exist when $0 \leq q \leq 2/3$. In particular, when $q < 2/3$ or, equivalently, $H_0 < 0.7071$, the solutions are smooth and even functions of θ. When $q = 2/3$ ($H_0 = 0.7071$), roughly speaking, there is too much liquid in the cylinder and a puddle of liquid forms in the quadrant $\left(-\frac{\pi}{2}, 0\right]$, whose location can be determined as a quadrature depending on the value of H_0 (39). In this lower-order theory, the puddles manifest themselves as shocks, while solutions without shocks can be shown to be neutrally stable (41). The addition of surface tension effects has the effect of smoothing the shocks and also provides a possible mechanism for instability (38–42), which is of interest in many practical situations.

Corner defects

Sometimes objects to be coated have cross sections composed of straight segments and curved arcs. In this case, an approximate theory can be formulated as described in Flow Over Nonflat Substances. Lubrication-type equations using this approach are capable of modeling the development of *corner defects*, such as the flow away from outside corners and puddling at inside corners (43). Fig. 4B (25) shows the flow history for an initally uniform coating that is applied to a substrate of square cross section with rounded corners of small radius, a wrought-iron fence post, for example. Surface tension causes rapid flow away from the corner. Final dry coating thicknesses may be expected to be small there. Indeed, failure of coatings at fence post edges is commonly observed.

It is possible, at least in principle, to mitigate this problem if a coating that developed Marangoni forces as it dries is used, as discussed in the next section. If the drying rate is selected appropriately, a virtually uniform final dry coating can be achieved.

Effects of Compositional Changes and Drying

Certain binary liquid mixtures have surface tension values that vary with the fractional composition. A commonplace example is an alkyd paint whose surface tension increases as the solvent evaporates. Strong surface tension gradient effects can arise for a thin, nonuniform coating layer of the mixture. Often there is surprising behavior; an initial hump in the coating may turn into a local depression in the final dry coating. An extended thin film model can reproduce such phenomena. Representative equations (44) are

$$\frac{\partial h}{\partial t} = -\nabla \cdot \left[\frac{h^2}{2\mu}\nabla\sigma + \frac{h^3}{3\mu}\nabla^2 h \nabla\sigma + \frac{h^3}{3\mu}\sigma\nabla\nabla^2 h - \frac{h^3}{3\mu}\rho g \nabla h \right] - E \tag{23}$$

$$\frac{\partial (ch)}{\partial t} = \nabla \cdot (Dh\nabla c - c\mathrm{Q}) \tag{24}$$

These two partial differential equations are solved simultaneously for the layer thickness, h, and the ''resin fraction,'' c. Additional relations are supplied that relate the viscosity, μ, the diffusivity, D, the surface tension, σ and the evaporation rate, E, of the solvent fraction. This simple drying model postulates a known relation between evaporation rate and local mixture composition. Admittedly, this is an oversimplification of the relevant thermodynamics.

Fig. 5 (44) shows two frames from the simulation of drying with developed surface tension gradient effect. Initial humps in the coating become depressions in the final dry coating, in agreement with experimental results (45).

Other Marangoni-Driven Flows

Surfactant or solute driven

If a surfactant is added to a liquid the surface tension becomes a function of the interfacial concentration, C, i.e., $\sigma = \sigma(C)$. All surfactants tend to be at least partly soluble in the bulk liquid and in general there will be a relationship between the surfactant adsorbed at the surface and the concentration in the bulk liquid. If this is a significant effect, the kinetics of adsorption must then be modeled, i.e., such cases must model the flow of liquid, the bulk concentration, and the concentration in the interface and

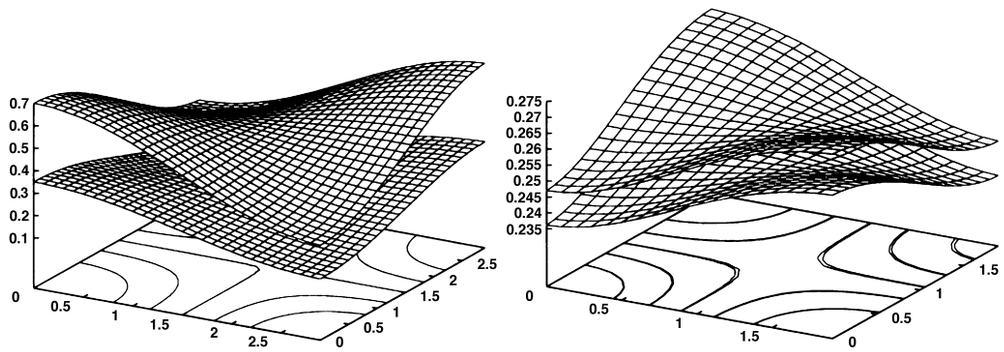

Fig. 5 The leveling of an uneven coating with compositional changes; Coating height and ''resin height'' are shown. *Left*: At beginning; *Right*: Nearly dry coating. The Marangoni effect causes initial humps to dry as depressions. (Reprinted with permission from Ref. 44 ©1999 American Chemical Society.)

we refer to such flows as solutal Marangoni driven. This distinguishes them from ''pure'' surfactant driven flows where the solubility can be neglected for modeling purposes and the surfactant is confined to the interface. However the flow dynamics in each case are very similar. There are many examples in the literature of the modeling of such processes, e.g., Ref. 46 but we will consider one particular limiting case here (23). An undisturbed thin film of water rests on a large horizontal substrate and a piece of cotton wool saturated with alcohol (e.g., *n*-butanol) is held above the free surface. The alcohol diffuses into the liquid film thus changing its surface tension. As the concentration of alcohol immediately below the source tends to be highest, the surface tension is lowest at this point and this gives rise to a shear stress which drives the flow. In the 2-D case (23), the evolution equation for the free surface $z = h(x, t)$ is

$$h_t = \frac{1}{2}(h^2\sigma_x)_x + \epsilon^2 B\left(\frac{1}{3}h^3 h_x\right)_x + \epsilon^2\sigma\left(\frac{1}{3}h^3 h_{xxx}\right)_x \tag{25}$$

where L is the distance from the source to the undisturbed liquid film, and $B = \rho g L^2/\chi$ where $\chi = \sigma_{\max} - \sigma_{\min}$ is the spreading pressure. We assume that the alcohol is fully soluble and that the bulk liquid and the interface are in quasi equilibrium. For a sufficiently thin liquid film, the alcohol concentration is approximately constant across the layer and the transport problem for the alcohol is uncoupled from the flow problem, i.e., the alcohol concentration in the gas (allowing for a partition coefficient) is impressed across the water film. In this case the concentration in the interface is given by

$$C(x,t) \approx \frac{2A}{t^*}\exp\frac{-(x^{*2}+1)P_1}{4t^*} \tag{26}$$

where $t^* = \chi Ht/\mu L^2$, $x^* = x/L$, A is the alcohol source strength, $P_1 = \chi H/D_g\mu$, and D_g is the diffusion constant for alcohol vapor in air. In Eq. 25 we thus consider $\sigma = \sigma(C) = \sigma(x, t)$. Eq. 25 is typical of many thin film flows: The flow is driven by the first-order terms while the $O(\epsilon^2 B, \epsilon^2)$ terms smooth the solution and prevent shock formation, which will otherwise inevitably occur. A typical computation is shown in Fig. 6A for the flow in an originally flat liquid film, i.e., $h(x, 0) = 1$.

Temperature gradient driven

Because surface tension generally decreases with increasing temperature, liquid motion can be driven by an imposed temperature gradient, $\partial T/\partial x$. If this gradient is assumed constant, a driving term of the form $1/(2\mu)\ \tau\ \partial(h^2)/\partial x$, where $\tau = (\partial\sigma/\partial T)(\partial T/\partial x)$, may be appended to the evolution equation. The resulting driven flow, analogous to one produced by wind shear, is known to be unstable and develops growing ''fingers.'' Fig. 6B shows a simulation (48) at a particular instant of time in agreement with experimental results (47).

This problem is closely related to fingering in draining flow on a vertical wall (49). Simulation results have also been compared with published linear stability analyses for the two problems (50). In each, the most unstable wavenumber and initial growth rates in the simulation are close to the predictions of the linear analyses.

Non-Newtonian Rheology

The equations can be extended to account for non-Newtonian flow behavior. There are many different models that propose relationships among the viscosity, stress, and strain rate. A particularly attractive choice is the Ellis model, which describes a liquid that, at low levels of stress,

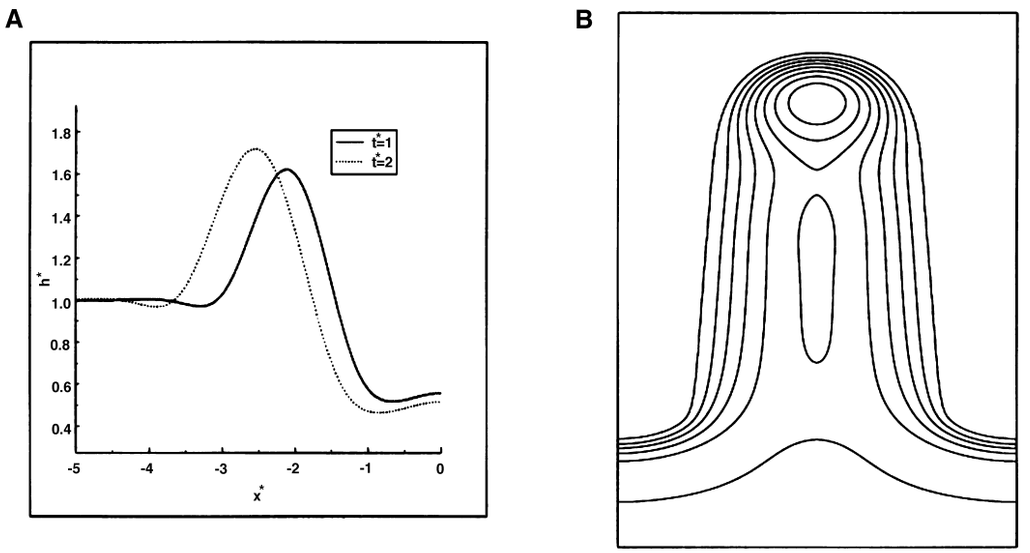

Fig. 6 (**A**) Marangoni drying flow induced by surfactant. (**B**) Simulation of thin-film ''fingering'' driven by a temperature gradient.

flows at constant viscosity, while at high stress levels displays power law, shear thinning behavior.

As a preliminary example, we show that the Ellis model can relieve the moving contact line singularity when a liquid moves onto a dry substrate. In contrast to previous models that allow contact line motion, it is no longer necessary to abandon the no-slip condition at the substrate in the vicinity of the contact point. While the stress is still unbounded at the contact point, the integrated stress or contact line force is finite. A three-constant Ellis viscosity model is employed which allows a low-shear Newtonian viscosity and may thus be used to model essentially Newtonian flows where shear-thinning only becomes important in the immediate vicinity of the contact point (8).

We consider the motion of a semi-infinite uniform coating layer draining down a previously dry, vertical substrate where x is measured downward along the wall, y is the normal coordinate, and $h(x)$ is the steady free-surface shape to be determined. The origin of coordinates is at $x = 0$ and the liquid-gas interface meets the wall at this point with an included angle θ_c. The wall is moving upward at a speed U, selected to render the motion steady. Far upstream of the contact point, the uniform liquid thickness is h_1.

For downward flow in a vertical wall, the shear stress in the liquid is

$$\tau = (\sigma h_{xxx} + \rho g)(h - y)$$

The liquid is assumed to obey an Ellis constitutive law (52)

$$\tau = \eta u_y$$

where

$$\frac{1}{\eta} = \frac{1}{\eta_0}\left(1 + \left|\frac{\tau}{\tau_{1/2}}\right|^{\alpha-1}\right) \tag{27}$$

Here, η is the viscosity, η_0 the viscosity at zero shear stress, $\tau_{1/2}$ the shear stress at which the viscosity is reduced by a factor of 1/2, and α is a power law index. When $\alpha = 1$, the liquid is Newtonian, while for $\alpha > 1$, the liquid is shear thinning. The Ellis viscosity model incorporates power law behavior at high shear stresses while allowing for a Newtonian plateau at low shear stresses. Because the free surface of the coating is stress free, and the shear stress in the liquid far away from the contact point is quite small, this is a particularly appropriate rheological model.

A speed, U, is selected so as to make the free surface steady in the moving coordinate system. In dimensionless variables, the ordinary differential equation satisfied by the liquid surface is

$$(h^*_{x^*x^*x^*} + 1)h^{*3}\left[1 + \frac{3}{\alpha+2}\left|(h^*_{x^*x^*x^*} + 1)Bh^*\right|^{\alpha-1}\right] = h^*\left[1 + \frac{3}{\alpha+2}B^{\alpha-1}\right] \tag{28}$$

where $h^* = h/h_1, x^* = [\rho g/((\sigma h_1)]^{1/3}x$, and $B = \rho g h_1/\tau_{1/2}$.

Eq. 28 can be solved by a shooting method, starting at a large distance upstream of the contact point, where $h^* \to 1$ as $x^* \to -\infty$. The additional boundary conditions on $h^*_{x^*}$ and $h^*_{x^*x^*}$ are derived from a linearized form

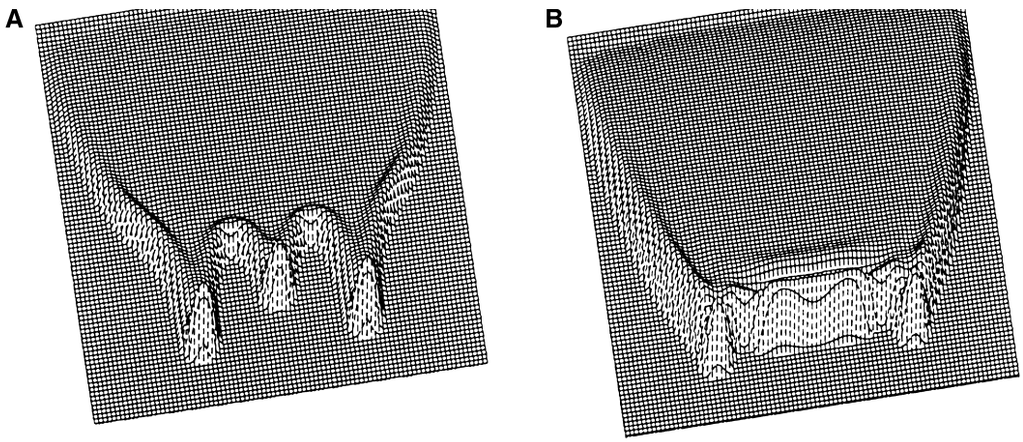

Fig. 7 (**A**) Sagging of a Newtonian coating showing pronounced drip marks. (**B**) Sagging of a shear-thinning coating. Drip marks are less developed.

of Eq. 28, appropriate to the far upstream region where the surface oscillation amplitude is very small (4). For a given set of up stream boundary conditions, the free surface profile equation is integrated numerically all the way to the contact point using a fourth-order Runge–Kutta scheme. The slope, where the free surface meets the substrate, and the maximum ''overshoot'' of the liquid layer, are found as part of the solution; they are, in general, functions of both the stress ratio, B, and the shear-thinning exponent; α. It may be verified that, while the wall shear stress becomes unbounded at the contact point, the total force is integrable, provided $\alpha > 1$. Weidner and Schwartz (8) also suggest reasons why nominally Newtonian liquids may shear thin at high levels of stress. Adiabatic viscous heating is known to cause a reduction in viscosity, for example. There is experimental evidence for such viscosity reduction at very high stresses for Newtonian liquids.

The introduction of somewhat more complex rheology into the multi dimensional lubrication model can be accomplished without difficulty and constitutes a useful generalization, even when contact line motion is not an issue. We consider, as an example, sagging resulting from ''overspray,'' when coating a vertical panel. ''Sagging'' refers here to the pattern of ''fingers'' or drip marks that often are observed when coating vertical surfaces. Once the coating has dried, sagging patterns typically form an unsightly defect; thus, a basic understanding of the mechanisms leading to drip marks will have important implications for the design of new coatings in order to minimize this effect. It is clear that surface tension contributes to defect formation. It is also known that the effect is less pronounced when the rheology is shear thinning, as compared to a Newtonian coating.

As the initial condition for the simulation, we consider a uniform thin coating on the vertical substrate. In addition there is a ''hyperellipsoidal'' mound with the equation $h(x, y) = h_0[1 - A(x - x_0)^4 - B(y - y_0)^4]^{1/4}$ superimposed on the uniform layer. A, B, x_0, and y_0 are constants specifying the major and minor axes of the mound and its center, respectively. The hyperellipsoid represents a thick overspray, perhaps applied inadvertently in practice. The simulation assumes a surface tension of 0.03 N m^{-1} and we take the thin coating layer to have a wet thickness of 0.02 cm, while the maximum height of the overspray mound is 0.4 cm. The parameters A and B are selected to make the width of the mound equal to 7.2 cm, while the width, in the downward direction, is 1.4 cm. The timescale is proportional to the viscosity μ; for $\rho g = 10^4$ Kg m^{-2} s^{-2}, and a Newtonian viscosity of 0.3 Kg m^{-1} s^{-1}, the characteristic time is $T \approx 1$ s.

Fig. 7A shows the fate of the initial overspray mound after 107 s have elapsed for the Newtonian coating. The figure shows developed drip marks and large capillary ridges at the troughs. By contrast, Fig. 7B is a simulation for a shear-thinning Ellis liquid, with exponent $\alpha = 2$ in the rheological Eq. 27. The liquid has advanced down the wall about the same distance; however, the drip marks are much less well developed.

CONCLUDING REMARKS

Thin film flows are of importance in manufacturing, basic studies in physics and chemistry, and the life sciences. As indicated here, mathematical approximation and numerical computation have achieved considerable success in modeling these flows leading to an improved understand-

ing of causal mechanisms. Such understanding can be expected to help in the formulation of new products and processes.

Here we have considered only flows on solid substrates; we note that there is a class of thin film flows where both sides of the liquid film are free, as in soap films and foams (51).

ACKNOWLEDGMENT

This work is supported by the ICI Strategic Research Fund, the State of Delaware, the NASA Microgravity Program, and the Strategic Research Fund of the Materials and Surface Science Institute, University of Limerick.

REFERENCES

1. Kistler, S.; Scriven, L.E. Coating Flows. In *Computational Analysis of Polymers*; Pearson, J., Richardson, S., Eds.; Barking Essex: England, Appl. Sci. 1983.
2. Slikkerveer, P.J.; van Lohuizen, E.P.; O'Brien, S.B.G. An implicit surface tension algorithm for surface tension dominated free and moving boundary problems. Numer. Methods Fluids **1995**, *22*, 851–868.
3. Benney, D.J. Long waves on liquid films. J. Math. Phys. **1966**, *45*, 150.
4. Tuck, E.O.; Schwartz, L.W. A numerical and asymptotic study of some third-order ordinary differential equations relevant to draining and coating flows. SIAM Rev. **1990**, *32*, 453–469.
5. Acheson, D.J. *Elementary Fluid Dynamics*; Clarendon Press: Oxford, 1990.
6. Batchelor, G.K. *An Introduction to Fluid Dynamics*; CUP: Cambridge, 1967.
7. Atherton, R.W.; Homsy, G.M. On the derivation of evolution equations for interfacial waves. Chem. Eng. Commun. **1976**, *2*, 57.
8. Weidner, D.E.; Schwartz, L.W. Contact-line motion of shear-thinning liquids. Phys. Fluids **1994**, *6*, 3535–3538.
9. Leenaars, A.F.M.; O'Brien, S.B.G. Particle removal by surface tension forces. Philips J. Res. **1989**, *44*, 183–209.
10. O'Brien, S.B.G.; van den Brule, B.H.A.A. A mathematical model for the cleansing of silicon substrates by fluid immersion. J. Colloid Interface Sci. **1989**, *144*, 210–221.
11. de Gennes, P.G. Wetting: statics and dynamics. Rev. Mod. Phys. **1985**, *57*, 827–863.
12. Huh, C.; Scriven, L.E. Hydrodynamic model of a steady movement of a solid/liquid/fluid contact line. J. Colloid Interface Sci. **1971**, *35*, 85–101.
13. Dussan, V.E.B. The moving contact line: the slip boundary condition. J. Fluid Mech. **1976**, *77*, 665.
14. O'Brien, S.B.G. Surface tension and contact angle problems in industry. J. Adhes. Sci. Technol. **1992**, *6*, 1037–1051.
15. O'Brien, S.B.G. The meniscus near a small sphere and its relationship to line pinning. J. Colloid Interface Sci. **1996**, *183*, 51.
16. Hocking, L.M. Rival contact-angle models and the spreading of drops. J. Fluid Mech. **1992**, *239*, 671–681.
17. Dussan, V.E.B.; Rame, E.; Garoff, S. On identifying the appropriate boundary conditions at a moving contact line: an experimental investigation. J. Fluid Mech. **1991**, *230*, 97–116.
18. Thompson, P.A.; Robbins, M.O. Simulations of contact line motion: slip and the dynamic contact angle. Phys. Rev. Lett. **1989**, *63*, 766–769.
19. Moriarty, J.A.; Schwartz, L.W. Dynamic considerations in the closing and opening of holes in thin liquid films. J. Colloid Interface Sci. **1993**, *161*, 335–342.
20. Spaid, M.A.; Homsy, G.M. Stability of Newtonian and viscoelastic dynamic contact lines. Phys. Fluids **1996**, *8*, 460–478.
21. Lelah, M.D.; Marmur, A.M. Spreading kinetics of droplets on glass. J. Colloid Interface Sci. **1981**, *82*, 518.
22. Tanner, L. The spreading of silicone oil drops on horizontal surfaces. J. Phys. D: Appl. Phys. **1979**, *12*, 1473–1484.
23. O'Brien, S.B.G. On Marangoni drying: non-linear waves in a thin film. J. Fluid Mech. **1993**, *254*, 649–670.
24. Hayes, M.; O'Brien, S.B.G.; Lammers, J.A. Green's function for flow over a small two dimensional topography. Phys. Fluids **2000**, *12*, 2845–2861.
25. Schwartz, L.W.; Weidner, D.E. Modeling of coating flows on curved surfaces. J. Eng. Math. **1995**, *29*, 91–103.
26. Mitlin, V.S.; Petviashvili, N.V. Nonlinear dynamics of dewetting: kinetically stable structures. Phys. Lett. A **1994**, *192*, 323–326.
27. Schwartz, L.W.; Eley, R.R. Simulation of droplet motion on low-energy and heterogeneous surfaces. J. Colloid Interface Sci. **1998**, *202*, 173–188.
28. Schwartz, L.W. Hysteretic effects in droplet motions on heterogeneous substrates. Langmuir **1998**, *14*, 3440–3453.
29. Zosel, A. Studies of the wetting kinetics of liquid drops on solid surfaces. Colloid Polym. Sci. **1993**, *271*, 680.
30. Manneville, P. *Dissipative Structures and Weak Turbulence*; Academic Press: Boston, 1990.
31. Taylor, G.I.; Michael, D.H. On making holes in a sheet of fluid. J. Fluid Mech. **1973**, *58*, 625–639.
32. Moriarty, J.A.; Schwartz, L.W. Effective slip in numerical calculations of moving-contact-line problems. J. Eng. Math. **1992**, *26*, 81–86.
33. Fermigier, M.; Limat, L.; Wesfreid, J.E.; Boudinet, P.; Quilliet, C. Two-dimensional patterns in Rayleigh-Taylor instability of a thin layer. J. Fluid Mech. **1992**, *236*, 349–383.
34. Schwartz, L.W. Unsteady Simulation of Viscous Thin-Layer Flows. In *Free-Surface Flows with Viscosity*; Tyvand, P.A., Ed.; Computational Mechanics Publ.: Southampton, 1998; 203–233.

35. O'Brien, S.B.G. Matched asymptotic expansions for the shape of a hole in a thin film. Q. Appl. Math. **1999**, *57*, 453–465.
36. O'Brien, S.B.G. Asymptotics of a pinhole. J. Colloid Interface Sci. **1997**, *191*, 514.
37. Weidner, D.E.; Schwartz, L.W.; Eres, M.H. Simulation of coating layer evolution and drop formation on horizontal cylinders. J. Colloid Interface Sci. **1997**, *187*, 243–258.
38. Moffat, H.K. Behaviour of a viscous film on the outer surface of a rotating cylinder. J. Mec. **1977**, *16*, 651.
39. O'Brien, S.B.G.; Gath, E.G. The location of a shock in rimming flow. Phys. Fluids **1998**, *10*, 1040.
40. Johnson, R.E. Steady state coating flows inside a rotating horizontal cylinder. J. Fluid Mech. **1988**, *190*, 321–342.
41. O'Brien, S.B.G. Linear stability of rimming flows. Q. Appl. Math. **2000**, *in press*.
42. O'Brien, S.B.G. A mechanism for instabilities in two dimensional rimming flow. Q. Appl. Math. **2000**, *in press.*
43. Weidner, D.E.; Schwartz, L.W.; Eley, R.R. Role of surface tension gradients in correcting coating defects in corners. J. Colloid Interface Sci. **1996**, *179*, 66–75.
44. Eres, M.H.; Weidner, D.E.; Schwartz, L.W. Three-dimensional direct numerical simulation of surface-tension-gradient effects on the leveling of an evaporating multicomponent fluid. Langmuir **1999**, *15*, 1859–1871.
45. Overdiep, W. The levelling of paints. Prog. Org. Coat. **1986**, *14*, 159–175.
46. Jensen, O.E.; Grotberg, J.B. Insoluble surfactant spreading on a thin viscous film; shock evolution and structure. J. Fluid Mech. **1992**, *240*, 259.
47. Cazabat, A.M.; Heslot, F.; Carles, P.; Troian, S.M. Hydrodynamic fingering instability of driven wetting films. Adv. Colloid Interface Sci. **1992**, *39*, 61–75.
48. Eres, M.H.; Schwartz, L.W.; Roy, R.V. Fingering instabilities of driven thin coating films. Phys. Fluids **1999**, *12*, 1278–1295.
49. Schwartz, L.W. Viscous flows down an inclined plane: instability and finger formation. Phys. Fluids **1989**, *A1*, 443–445.
50. Kataoka, D.E.; Troian, S.M. A theoretical study of instabilities at the advancing front of thermally driven coating films. J. Colloid Interface Sci. **1997**, *192*, 350–362.
51. Schwartz, L.W.; Roy, R.V. Modeling draining flow in mobile and immobile soap films. J. Colloid Interface Sci. **1999**, *218*, 309–323.
52. Byrd, R.B.; Armstrong, R.C.; Hassager, O. *Dynamics of Polymeric Liquids*; Wiley: New York, 1977; Vol. 1.